HHS Public Access

Author manuscript

JAMA Dermatol. Author manuscript; available in PMC 2016 October 01.

Published in final edited form as:

JAMA Dermatol. 2015 October 1; 151(10): 1068–1074. doi:10.1001/jamadermatol.2015.0453.

In Vivo Multiphoton Microscopy of Basal Cell Carcinoma

Mihaela Balu, PhD,
Laser Microbeam and Medical Program, Beckman Laser Institute, University of California–Irvine, Irvine

Christopher B. Zachary, MD,
Department of Dermatology, University of California–Irvine, Irvine

Ronald M. Harris, MD,
Department of Dermatology, University of California–Irvine, Irvine

Tatiana B. Krasieva, PhD,
Laser Microbeam and Medical Program, Beckman Laser Institute, University of California–Irvine, Irvine

Karsten König, PhD,
JenLab GmbH, Jena, Germany; Department of Biophotonics and Laser Technology, Saarland University, Saarbrücken, Germany

Bruce J. Tromberg, PhD, and
Laser Microbeam and Medical Program, Beckman Laser Institute, University of California–Irvine, Irvine

Kristen M. Kelly, MD
Department of Dermatology, University of California–Irvine, Irvine

Abstract

Importance—Basal cell carcinomas (BCCs) are diagnosed by clinical evaluation, which can include dermoscopic evaluation, biopsy, and histopathologic examination. Recent translation of

Corresponding Author: Kristen M. Kelly, MD, Department of Dermatology, University of California–Irvine, 1002 Health Sciences Rd, Irvine, CA 92612 (kmkelly@uci.edu).

Supplemental content at jamadermatology.com

Author Contributions: Dr Balu had full access to all of the data in the study and takes responsibility for the integrity of the data and the accuracy of the data analysis.
Study concept and design: Balu, Zachary, Krasieva, König, Tromberg, Kelly.
Acquisition, analysis, or interpretation of data: Balu, Zachary, Harris, Krasieva, Tromberg, Kelly.
Drafting of the manuscript: Balu, Zachary.
Critical revision of the manuscript for important intellectual content: All authors.
Statistical analysis: Harris.
Obtained funding: Tromberg.
Administrative, technical, or material support: Zachary, Krasieva, König, Tromberg.
Study supervision: Zachary, Tromberg, Kelly.

Conflict of Interest Disclosures: Dr König is cofounder of JenLab GmbH (Jena, Germany).

Previous Presentation: This article was presented at the American Society for Laser Medicine & Surgery Annual Conference; April 24, Kissimmee, Florida.

multiphoton microscopy (MPM) to clinical practice raises the possibility of noninvasive, label-free in vivo imaging of BCCs that could reduce the time from consultation to treatment.

Objectives—To demonstrate the capability of MPM to image in vivo BCC lesions in human skin, and to evaluate if histopathologic criteria can be identified in MPM images.

Design, Setting, and Participants—Imaging in patients with BCC was performed at the University of California–Irvine Health Beckman Laser Institute & Medical Clinic, Irvine, between September 2012 and April 2014, with a clinical MPM-based tomograph. Ten BCC lesions were imaged in vivo in 9 patients prior to biopsy. The MPM images were compared with histopathologic findings.

Main Outcomes and Measures—MPM imaging identified in vivo and noninvasively the main histopathologic feature of BCC lesions: nests of basaloid cells showing palisading in the peripheral cell layer at the dermoepidermal junction and/or in the dermis.

Results—The main MPM feature associated with the BCC lesions involved nests of basaloid cells present in the papillary and reticular dermis. This feature correlated well with histopathologic examination. Other MPM features included elongated tumor cells in the epidermis aligned in 1 direction and parallel collagen and elastin bundles surrounding the tumors.

Conclusions and Relevance—This study demonstrates, in a limited patient population, that noninvasive in vivo MPM imaging can provide label-free contrast that reveals several characteristic features of BCC lesions. Future studies are needed to validate the technique and correlate MPM performance with histopathologic examination.

Basal cell carcinoma (BCC) is a form of skin cancer originating from the basal cell layer of the epidermis and associated follicular structures. It is the most common human cancer, accounting for 25% of all cancer cases and 75% of skin malignant neoplasms diagnosed in the United States.[1] More than 2 million new nonmelanoma skin cancers are estimated to have been diagnosed in United States in 2014.[2] Basal cell carcinomas are diagnosed primarily by clinical evaluation. Furthermore, an increasing number of clinicians are being trained in the art of dermoscopy to aid in the diagnosis of early tumors. The definitive diagnosis has always been provided by a skin biopsy followed by sample preparation and histopathologic examination.

Advances in optical imaging and spectroscopy technologies raise the possibility of performing rapid and noninvasive light-based histopathologic examination, a pain-free process that would be appreciated by patients and reduce the time from consultation to treatment. Therefore, technologies such as conventional optical coherence tomography (OCT),[3,4] high-definition OCT (HD-OCT),[5-7] reflectance confocal microscopy (RCM),[8-15] multiphoton microscopy (MPM),[16,17] fluorescence lifetime microscopy (FLIM),[13,18] and multimodal spectral approaches[19] have been investigated for their applicability for diagnosis of skin cancer, including BCC. Each of these techniques has strengths and limitations that at present make them complementary.

Both OCT and HD-OCT have the benefit of deeper penetration (several hundreds of microns) compared with the microscopy techniques. However, although HD-OCT offers improved resolution compared with conventional OCT, it still proves insufficient in the

assessment of the cellular morphologic characteristics in tumor nests, which is important for accurate diagnosis of BCC. The microscopy laser-scanning techniques—RCM, MPM, and FLIM—have the ability to produce submicron resolution images. They are based on different contrast mechanisms, which is reflected in their capability to distinguish particular molecular compounds in the images. Among these techniques, FLIM, the contrast mechanism of which is based on differences in the fluorescence lifetime of different biomolecules in tissue, is the most efficient in distinguishing different endogenous fluorophores, such as bound and free components of nicotinamide adenine dinucleotide (NADH)and flavin adenine dinucleotide (FAD), keratin, melanin, porphyrin, elastin, and collagen. Distinguishing bound from free NADH-FAD is key in studying potential disease biomarkers related to cellular metabolism. To date, this technique has been explored only in ex vivo imaging of BCC in human skin.[13,18] Unlike FLIM, RCM is not able to distinguish different tissue fluorophores because its contrast mechanism is based on variation of tissue refractive index. In this technique, the light focused and raster-scanned on the skin surface is reflected and, on detection, reconstructed into a gray-scale image. Stacks of images are acquired at progressive depths in skin by adjustment of focus. This is a simple and efficient technique for obtaining 3-dimensional submicron resolution images of skin, but it has the disadvantage of not distinguishing among different tissue fluorophores. Generally, gray-scale images are sufficient for the overall assessment of the tissue structure, but in some cases, owing to its contrast mechanism, certain cellular structures, such as those inside the BCC tumor nests, are difficult to distinguish by RCM, and other criteria are usually introduced for BCC diagnosis.

The histopathologic characteristics of BCC are related to the presence in the dermis or at the dermoepidermal junction of islands of basaloid cells, often showing palisading in the peripheral cell layer.[20] The BCC tumor islands are referred to as “dark tumor islands,” “phantom islands,”[13] or “dark silhouettes”[15,21] in RCM imaging. This has been shown to lead to misdiagnosis of BCC by RCM.[21] Correct diagnosis of BCC requires an accurate assessment of both cellular morphologic characteristics inside the tumor nests as well as a low-power view of the nests overall.

Multiphoton microscopy selectively visualizes the cellular and extracellular matrix based on 2-photon excited fluorescence (TPEF) from NADH, FAD, melanin, keratin, and elastin fibers and on second-harmonic generation (SHG) from collagen fibers. Although the resolutions of RCM and MPM are comparable, MPM's contrast mechanism seems to favor visualization of certain cellular tissue structures. The cellular structures inside the BCC tumor are of interest and particularly discussed in this study. Multiphoton microscopy has been used in pilot studies on ex vivo[16] and recently on in vivo[17] imaging of BCC, but the BCC tumor nests were either not shown as being imaged[17] or their cellular structure was not resolved.[16]

In this study, we sought to assess the ability of the MPM to visualize the BCC tumor nests and their cellular structure. Compared with the previous pilot study,[17] this work was facilitated by using a recently developed clinical multiphoton to-mograph (MPTflex; JenLab GmbH). This is the successor model of JenLab's DermaInspect system.[22] It is a portable

instrument with an articulated arm, which allowed us to image lesions on different parts of the body rather than being limited to lesions on the extremities.[17]

Methods

Patients

This study included 10 BCC lesions imaged in 9 patients, the diagnoses of which were subsequently confirmed by standard histologic examination. Lesions that were hyperkeratotic, crusted, or ulcerated and those that had previously been biopsied were excluded. The topographic location and pathologic characteristics of each case are summarized in the Table. All in vivo measurements were conducted according to an approved institutional review board protocol of the University of California–Irvine (HS No. 2011-8494) with written informed consent obtained from all patients. Patients were compensated for their participation.

MPM-Based Clinical Tomograph MPTflex

Multiphoton microscopy is a laser-scanning microscopic technique that relies on nonlinear light-matter interactions, such as TPEF and SHG to achieve 3-dimensional submicron resolution images of tissue. In MPM, TPEF derives its signal from various sources, including NADH, FAD, keratin, melanin, and elastin fibers, whereas SHG is used to visualize collagen fibers. It is important to note that these contrast mechanisms rely on the intrinsic optical properties of endogenous tissue biomolecules without using specific fluorescent labels.

In this study, we used an MPM-based clinical tomograph (MPTflex) for imaging of BCC lesions in human skin. This system, as shown in Figure 1, consists of a compact, turn-key femtosecond (fs) laser (MaiTai Ti:Sappire oscillator, sub–100 fs, 80 MHz, tunable 690-1020 nm; Spectra Physics), an articulated arm with near-infrared optics, and beam-scanning module. The imaging head includes 2 photomultiplier tube (PMT) detectors used for parallel acquisition of TPEF and SHG signals. Owing to the high sensitivity of the detectors, the images were acquired in a darkened room. A customized metallic ring taped on the patient's skin attaches magnetically to the objective holder in the articulated arm, minimizing motion artifacts. The excitation wavelength used for this study was 790 nm. The TPEF signal was detected over the spectral range of 410 to 650 nm, whereas the SHG signal was detected over a narrow spectral bandwidth (385-405 nm) through emission filters placed in the TPEF and SHG detection channels, respectively. We used a Zeiss objective (40×, 1.3 numerical aperture, oil immersion) for focusing into the tissue. The laser power used was 5 mW at the surface of the skin and up to 30 mW in deeper skin layers. The articulated arm of the clinical tomograph allows imaging of almost any part of the body. However, some areas in proximity of the eyes, nose, or ears are still difficult to image.

Study Design

We acquired the MPM images using 2 scanning modalities: The first modality was x-y scanning, resulting in z-stacks of horizontal images from the stratum corneum to the dermis. The z-stacks were obtained by moving the objective in the z-direction, thus scanning at

different depths in the skin. The field of view for each optical section was about 200 × 200 μm^2. Typically, we set a step of 5 μm between the optical sections. Because the optical section is limited to a small scan field, the overall investigation of the lesion required the acquisition of several image stacks of different skin sites. We acquired about 3 image stacks for each lesion. The second modality was x-z scanning, resulting in cross-sectional, "histology-like" images from the stratum corneum to superficial dermis.

The x-y sections were 512 × 512–pixel images acquired at approximately 6 seconds per frame. The x-z sections were 1024 × 1024–pixel images acquired at approximately 30 seconds per frame. Owing to time constraints, we did not acquire x-z sections for all the lesions. This did not influence the results, however, because, the MPM features were clearly identified in the horizontal sections. For the same reason, we did not acquire images of normal skin adjacent to the lesion. Certainly, this would be necessary if the lesion margins are assessed, but this was not the purpose of our study.

Multiphoton microscopy imaging was performed in vivo prior to biopsy. All lesions suspected to be BCC through clinical dermatologic assessment were biopsied and diagnosed using standard hematoxylin-eosin histopathologic protocol.

Results

Nine patients with a total of 10 BCCs underwent imaging shortly before excisional surgery. The histopathologic features of these lesions are listed in the Table and included superficial, nodular, and micronodular BCCs. The main histopathologic findings were nests of basaloid cells extending along the dermoepidermal junction into the papillary dermis (superficial BCC) and various-sized nests invading the reticular dermis (nodular and micronodular BCC). The main MPM features associated with these lesions included (1) nests of basaloid cells present in the papillary and upper reticular dermis, some of which showed palisading in the peripheral cell layer; (2) elongated tumor cells in epidermis aligned in 1 direction; and (3) parallel collagen and elastin bundles surrounding the tumors. A summary of the MPM features found in each lesion is presented in the Table. The morphologic MPM features and the routine histologic findings corresponding to 3 of the 10 lesions are illustrated in Figures 2, 3, and 4). In addition, MPM images and histologic findings corresponding to a micronodular BCC lesion are presented in the eFigure in the Supplement.

Representative MPM images corresponding to 1 of the lesions are shown in Figure 2. A nest of basaloid cells can be seen in both horizontal sections (x-y scan) and the corresponding cross-sectional (x-z scan) images. Particularly in this lesion, the mucinous stroma adjacent to tumor was visualized with MPM. In the standard hematoxylin-eosin–stained histologic appearance, the stroma frequently shows retraction from the tumor islands because mucin shrinks during the process of fixation and dehydration of the specimen, so that the tumor islands appear partially or completely detached from the surrounding dermis.[23] The arrowheads in the images of Figure 2 indicate the mucin adjacent to tumor in the MPM images and its appearance as retraction from tumor islands in the histologic section. Histologic examination revealed palisading of peripheral layers in some of the tumor nests of the lesion, although this feature was not obvious in the nests imaged with MPM.

Representative MPM images acquired in a second lesion are presented in Figure 3 along with the corresponding histologic section.The MPM images of this lesion show tumor elongated cells aligned in 1 direction (Figure 3B). Palisading of the peripheral layer was present in the MPM images of the BCC nests of this lesion (Figure 3D).

Figure 4 shows the MPM images and the routine histologic findings corresponding to another lesion. The MPM images show the third feature we observed in this study: parallel bundles of collagen surrounding tumor masses, along with palisading of the peripheral cell layer, and tumor cells aligned in 1 direction. The bright cells in Figure 4D and E are most likely melanophages.

Discussion

In this study, we evaluated the potential of MPM to be used as a noninvasive in vivo imaging tool for the immediate and rapid diagnosis of BCC.

The main feature identified in all lesions by MPM imaging was the presence of nested groups of basaloid cells in the papillary and upper reticular dermis. Some of these nests showed palisading at the peripheral cell layer. This feature correlated well with the standard hematoxylin-eosin–stained histologic appearance of near-matching locations. Basal cell carcinoma tumor nests have been previously imaged with various optical imaging techniques.[3-7,9,13-18] The morphologic structures inside the tumor nests were clearly observed only in 2 reported studies[13,18] on ex vivo imaging of BCC in human skin using FLIM. Our study shows that in vivo MPM imaging can resolve the cellular structure inside the tumor nests corresponding to BCC lesions that include superficial components. This is important because the presence of nests of basaloid cells at the dermoepidermal junction and/or in the dermis is the main histopathologic criterion for BCC diagnosis.[20] Therefore, this feature can be potentially used as a criterion for BCC diagnosis with MPM imaging. It still remains challenging to resolve the cellular structure of deeper nests, such as ones found in micronodular BCC (eFigure in the Supplement), but this needs to be investigated in an extended study to include a larger number of nodular and micronodular BCC lesions.

Elongated cells, oriented in 1 direction in the epidermis, have been previously identified in BCC lesions by in vivo RCM[8,10,11,13,14] and ex vivo MPM imaging,[13,16] although in the latter study[16] this was present in only 1 of 6 tumors. This feature has traditionally been considered an RCM criterion for in vivo diagnosis of BCC because it was identified with high sensitivity and specificity in these lesions.[10] While in some studies the elongated cells, oriented in 1 direction are regarded as BCC tumoral cells[8,11] or BCC tumoral palisading,[10] in others, they were referred to as keratinocytes and most likely regarded as epidermal response to underlying BCC.[13,16] In this study, we imaged elongated cells oriented in 1 direction in 4 of 10 lesions. All these lesions were superficial BCCs or nodular BCCs with superficial components. We believe that the presence of elongated cells oriented in a single direction can be explained as appearing only in those BCCs that are superficial enough to be imaged in the epidermis and not, as previously stated,[13,16] to be a specific (pathognomonic) feature present in the overlying epidermis of underlying BCCs. If present, elongated cells are related to the palisading of the peripheral cell layer in the intraepidermal BCC nests of

basaloid cells. Nevertheless, in 1 of the 4 lesions, the elongated cells oriented in a single direction were present in very superficial layers of the epidermis (Figure 3B). The standard hematoxylin-eosin– stained histologic appearance corresponding to this lesion did not show the presence of this feature in the upper epidermal layers. However, the sampling of heterogeneous tumor will inevitably be somewhat imprecise when attempting to correlate with standard histologic appearance. Horizontal rather than vertical hematoxylin-eosin–stained sections might be more effective in correlating this phenomenon provided by MPM imaging with histologic appearance.

It is well established that islands of tumor are surrounded by a proliferating connective tissue stroma, which is arranged in parallel bundles surrounding the tumor masses so that a relationship seems to exist between the tumor and its stroma.[23,24] We found this interesting feature in 5 of the 10 BCC lesions imaged. Parallel bundles of collagen and elastin around the tumor masses have been previously noted in an RCM imaging study of BCC lesions.[9] In a previous study,[24] the tumor-induced stroma of BCC was associated with the superficial subtype of this tumor. However, in our study, this feature did not indicate a predilection for a particular subtype. Stroma morphologic characteristics of BCC lesions should be further investigated in future studies with larger number of patients.

In this study, we demonstrate that MPM is capable of imaging in vivo tumor nests in BCC lesions of superficial and nodular types along with other features that may be specific to BCC. The MPM imaging was able to visualize the cellular structure inside the tumor nests of BCC lesions that included superficial components. These results provide the groundwork for a future study with a larger number of patients that would assess MPM imaging sensitivity and specificity for in vivo noninvasive BCC diagnosis. One might foresee 2 major technical limitations in performing such a study. In this early stage of MPM clinical translation, limited field of view (about 250 × 250 μm^2) and penetration depth (about 200-300 μm) are the main technical challenges. High penetration depth is important for imaging tumor nests that are far from the dermoepidermal junction in the dermis, as is often the case for nodular BCC. One way to increase penetration depth is implementing dispersion compensation to decrease the laser pulse duration,[25] but the gain would be limited. Nevertheless, MPM imaging of tumor nests in several nodular BCC included in this work shows great promise. Scanning large areas of the lesions is important to avoid false-negative diagnoses because lesions are often nonuniform, presenting focal dysplasia and/or malignant neoplasm. The field of view can be increased by implementing a mosaic feature (acquisition of adjacent field of views) or by redesign of the optical components. This technical limitation is being addressed, and implementation has been initiated in a newly developed instrument.

Conclusions

This study demonstrates, in a limited patient population, that noninvasive in vivo MPM imaging can provide label-free contrast that reveals several characteristic features of BCC lesions. Future studies are needed to validate the technique and correlate MPM performance with histopathologic findings.

Supplementary Material

Refer to Web version on PubMed Central for supplementary material.

Acknowledgments

Funding/Support: This study was supported in part by the following grants: National Institutes of Health (NIH) NIBIB Laser Microbeam and Medical Program (LAMMP, P41-EB015890), NCI-2P30CA62203 (University of California–Irvine Cancer Center Support Grant), NIH K25-EB007309, and Air Force Research Laboratory Agreement No. FA9550-04-1-0101 and by the Beckman Laser Institute programmatic support from the Arnold and Mabel Beckman Foundation.

Role of the Funder/Sponsor: The sponsors had no role in the design and conduct of the study; in the collection, analysis, and interpretation of data; or in the preparation, review, or approval of the manuscript.

References

1. Reszko, A.; Wilson, LD.; Leffell, DJ. Cancer of the skin. In: DeVita, VT.; Lawrence, TS.; Rosenberg, SA., editors. DeVita, Hellman, and Rosenberg's Cancer: Principles & Practice of Oncology. 9th. Philadelphia, PA: Lippincott Williams & Wilkins; 2011. p. 1610-1616.
2. National Cancer Institute. [Accessed May 10, 2014] Skin cancer. http://www.cancer.gov/cancertopics/types/skin
3. Olmedo JM, Warschaw KE, Schmitt JM, Swanson DL. Optical coherence tomography for the characterization of basal cell carcinoma in vivo: a pilot study. J Am Acad Dermatol. 2006; 55(3): 408–412. [PubMed: 16908344]
4. Gambichler T, Orlikov A, Vasa R, et al. In vivo optical coherence tomography of basal cell carcinoma. J Dermatol Sci. 2007; 45(3):167–173. [PubMed: 17215110]
5. Boone MA, Norrenberg S, Jemec GB, Del Marmol V. Imaging of basal cell carcinoma by high-definition optical coherence tomography: histomorphological correlation: a pilot study. Br J Dermatol. 2012; 167(4):856–864. [PubMed: 22862425]
6. Maier T, Braun-Falco M, Hinz T, Schmid-Wendtner MH, Ruzicka T, Berking C. Morphology of basal cell carcinoma in high definition optical coherence tomography: en-face and slice imaging mode, and comparison with histology. J Eur Acad Dermatol Venereol. 2013; 27(1):e97–e104. [PubMed: 22540280]
7. Gambichler T, Plura I, Kampilafkos P, et al. Histopathological correlates of basal cell carcinoma in the slice and en face imaging modes of high-definition optical coherence tomography. Br J Dermatol. 2014; 170(6):1358–1361. [PubMed: 24359160]
8. González S, Tannous Z. Real-time, in vivo confocal reflectance microscopy of basal cell carcinoma. J Am Acad Dermatol. 2002; 47(6):869–874. [PubMed: 12451371]
9. Sauermann K, Gambichler T, Wilmert M, et al. Investigation of basal cell carcinoma [correction of carcionoma] by confocal laser scanning microscopy in vivo. Skin Res Technol. 2002; 8(3):141–147. [PubMed: 12236882]
10. Nori S, Rius-Díaz F, Cuevas J, et al. Sensitivity and specificity of reflectance-mode confocal microscopy for in vivo diagnosis of basal cell carcinoma: a multicenter study. J Am Acad Dermatol. 2004; 51(6):923–930. [PubMed: 15583584]
11. Marra DE, Torres A, Schanbacher CF, Gonzalez S. Detection of residual basal cell carcinoma by in vivo confocal microscopy. Dermatol Surg. 2005; 31(5):538–541. [PubMed: 15962737]
12. Guitera P, Menzies SW, Longo C, Cesinaro AM, Scolyer RA, Pellacani G. In vivo confocal microscopy for diagnosis of melanoma and basal cell carcinoma using a two-step method: analysis of 710 consecutive clinically equivocal cases. J Invest Dermatol. 2012; 132(10):2386–2394. [PubMed: 22718115]
13. Manfredini M, Arginelli F, Dunsby C, et al. High-resolution imaging of basal cell carcinoma: a comparison between multiphoton microscopy with fluorescence lifetime imaging and reflectance confocal microscopy. Skin Res Technol. 2013; 19(1):e433–e443. [PubMed: 22970856]

14. Longo C, Lallas A, Kyrgidis A, et al. Classifying distinct basal cell carcinoma subtype by means of dermatoscopy and reflectance confocal microscopy. J Am Acad Dermatol. 2014; 71(4):716–724.e1. [PubMed: 24928707]

15. González S, Sánchez V, González-Rodríguez A, Parrado C, Ullrich M. Confocal microscopy patterns in nonmelanoma skin cancer and clinical applications. Actas Dermosifiliogr. 2014; 105(5):446–458. [PubMed: 24002008]

16. Paoli J, Smedh M, Wennberg AM, Ericson MB. Multiphoton laser scanning microscopy on non-melanoma skin cancer: morphologic features for future non-invasive diagnostics. J Invest Dermatol. 2008; 128(5):1248–1255. [PubMed: 17989735]

17. Ulrich M, Klemp M, Darvin ME, König K, Lademann J, Meinke MC. In vivo detection of basal cell carcinoma: comparison of a reflectance confocal microscope and a multiphoton tomograph. J Biomed Opt. 2013; 18(6):61229. [PubMed: 23456144]

18. Patalay R, Talbot C, Alexandrov Y, et al. Multiphoton multispectral fluorescence lifetime tomography for the evaluation of basal cell carcinomas. PLoS One. 2012; 7(9):e43460. [PubMed: 22984428]

19. Lim L, Nichols B, Migden MR, et al. Clinical study of noninvasive in vivo melanoma and nonmelanoma skin cancers using multimodal spectral diagnosis. J Biomed Opt. 2014; 19(11): 117003. [PubMed: 25375350]

20. McKee, PH.; Calonje, E.; Granter, SR. Basal Cell Carcinoma. 3rd. Vol. 2. St Louis, MO: Mosby; 2005. p. 1167-1184.

21. Cinotti E, Perrot JL, Campolmi N, et al. The role of in vivo confocal microscopy in the diagnosis of eyelid margin tumors: 47 cases. J Am Acad Dermatol. 2014; 71(5):912–918.e2. [PubMed: 24998093]

22. Konig K, Riemann I. High-resolution multiphoton tomography of human skin with subcellular spatial resolution and picosecond time resolution. J Biomed Opt. 2003; 8(3):432–439. [PubMed: 12880349]

23. Lever, WF. Histopathology of the Skin. 6th. Philadelphia, PA: J. B. Lippincott Co; 1983.

24. Pinkus H. Epithelial and fibroepithelial tumors. Bull N Y Acad Med. 1965; 41:176–189. [PubMed: 14232145]

25. Tang S, Krasieva TB, Chen Z, Tempea G, Tromberg BJ. Effect of pulse duration on two-photon excited fluorescence and second harmonic generation in nonlinear optical microscopy. J Biomed Opt. 2006; 11(2):020501. [PubMed: 16674172]

Figure 1. The Imaging Procedure of a Skin Lesion on the Face

Using the multiphoton microscopy (MPM)-based clinical tomograph (MPTflex).

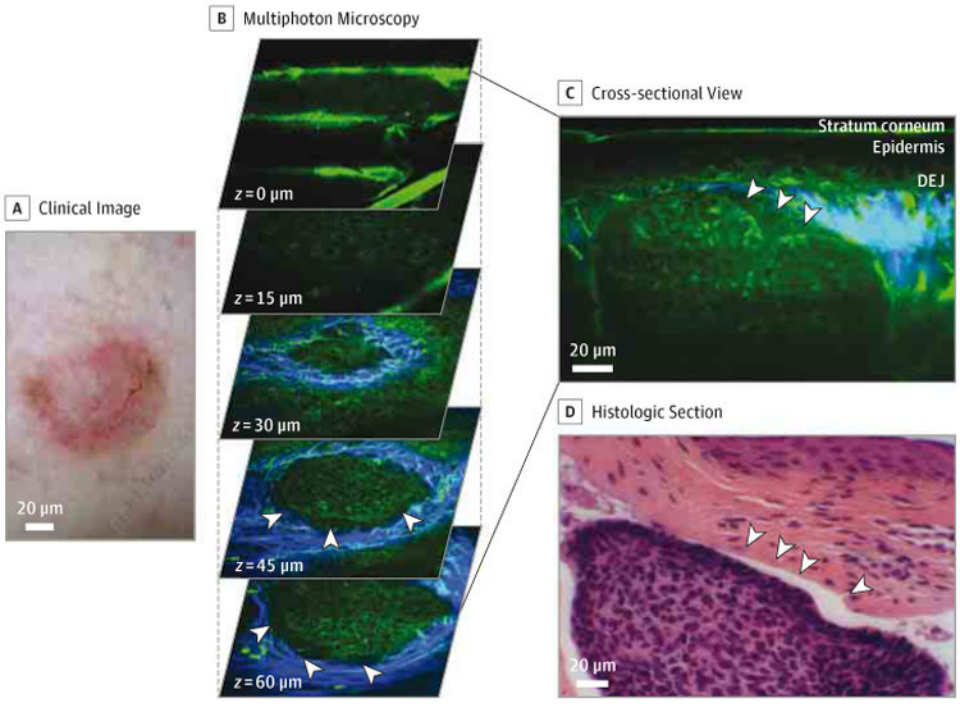

Figure 2. Basal Cell Carcinoma (BCC) (Superficial and Nodular Components)

A, Clinical image (DermLite FOTO, DermLite Inc). B, Multiphoton microscopy (MPM) en-face images (x-y scans) of the stratum corneum at z = 0 µm, of keratinocytes in the stratum spinosum at z = 15 µm, of a nest of basaloid cells (green) surrounded by collagen (blue) and elastin fibers (green) imaged at different depths: z = 30 µm, 45 µm, and 60 µm. C, Cross-sectional view (x-z scan) corresponding to a vertical plane through the same interrogating volume shown on the left. DEJ indicates dermo-epidermal junction. D, Hematoxylin-eosin–stained histologic section of the lesion; original magnification ×40. Both the MPM and the histologic images show a mucinous stroma adjacent to the tumor mass (case 2). B-D, Arrowheads indicate mucinous stroma.

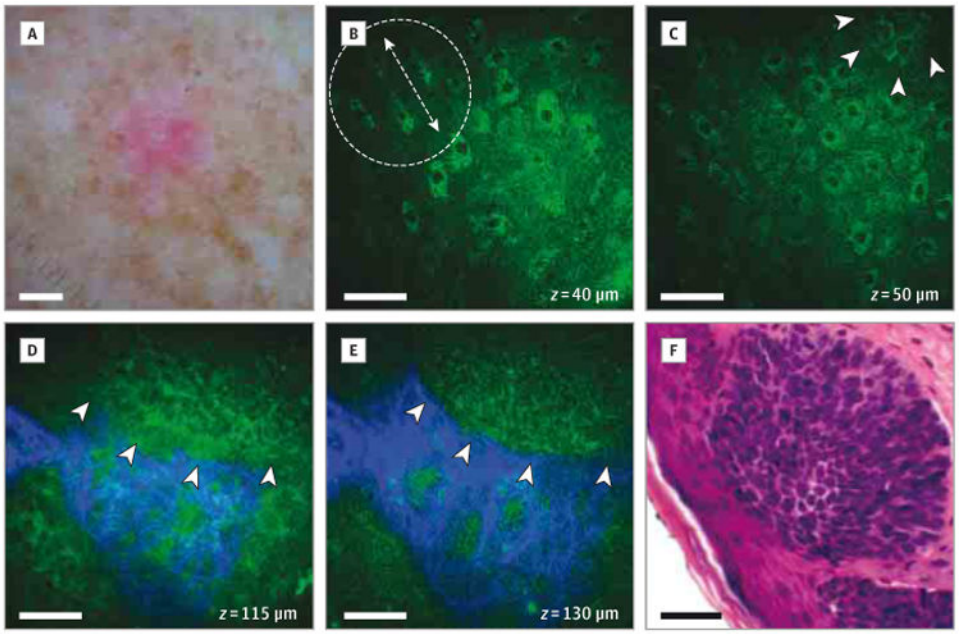

Figure 3. Superficial Basal Cell Carcinoma (BCC)

A, Clinical image (DermLite FOTO, DermLite Inc). Scale bar is 2 mm. B, Multiphoton microscopy (MPM) image of the stratum spinosum (dashed circle) (z = 40 µm) showing tumor elongated cells aligned in 1 direction (arrow) in the epidermis. C, MPM image of the lower epidermis (z = 50 µm) showing the tip of a tumor BCC nest (arrowheads) attached to the undersurface of the epidermis. D, MPM image of the same nest (arrowheads) showing palisading in the peripheral cell layer. This image represents a z-projection of 3 consecutive images (3-µm step) for an increase in the depth of field and better visualization. E, MPM image of the same nest in a deeper layer (arrowheads) (z = 130 µm). F, Hematoxylin-eosin–stained histologic section of the lesion; original magnification ×40. B-F, Scale bar is 40 µm (case 1).

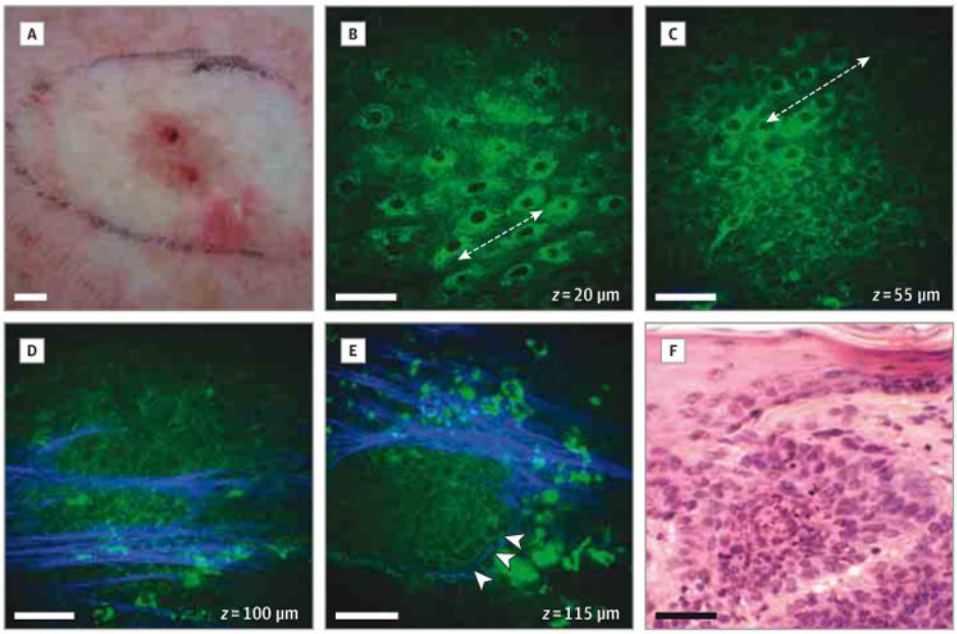

Figure 4. Nodular and Superficial Basal Cell Carcinoma (BCC)

A, Clinical image (DermLite FOTO, DermLite Inc). Scale bar is 2 mm. B, Multiphoton microscopy (MPM) image of the stratum granulosum (z = 20 µm) showing elongated tumor cells aligned in 1 direction (arrow). C, MPM image of the lower epidermis (z = 50 µm) showing tumor cells aligned in 1 direction (arrow). D, MPM image showing parallel collagen fibers (blue) on top of tumor. E, MPM image showing parallel collagen fibers surrounding a BCC tumor nest. Arrowheads indicate palisading in the peripheral cell layer. F, Histologic section of the lesion (hematoxylin-eosin, original magnification ×40). B-F, Scale bar is 40 µm (case 9).

Table

Location of the Lesions, Pathologic Diagnosis, and MPM Morphologic Features of BCC

			Morphologic Features		
Case No.	Location	Pathological Diagnosis	Nests of Basaloid Cells in the Papillary and/or Upper Dermis	Elongated Tumor Cells Aligned in 1 Direction	Parallel Collagen and Elastin Bundles
1	Thigh	SBCC	+	+	−
2	Shoulder	SBCC + NBCC	+	−	+
3	Arm	SBCC	+	−	−
4	Shoulder	SBCC	+	+	+
5	Back	SBCC	+	−	+
6	Back	NBCC	+	−	−
7	Face	MNBCC + NBCC	+	−	+
8	Leg	SBCC	+	+	−
9	Arm	SBCC + NBCC	+	+	+
10	Arm	SBCC	+	−	−

Abbreviations: BCC, basal cell carcinomas; MNBCC, micronodular BCC; MPM, multiphoton microscopy; NBCC, nodular BCC; SBCC, superficial BCC; +, present; −, absent.